Research Square

Preprints are preliminary reports that have not undergone peer review.
They should not be considered conclusive, used to inform clinical practice,
or referenced by the media as validated information.

Integrated Ambulatory Blood Pressure, Electrocardiographic, and Inflammatory Markers for Cross-sectional Discrimination of Echocardiographically Defined Left Ventricular Diastolic Dysfunction

Ayhan Cosgun

drcard1234@gmail.com

Cihanbeyli State Hospital

Huseyin Oren

Ankara Bilkent City Hospital

Research Article

Keywords: ambulatory blood pressure monitoring, diastolic morning surge, left ventricular diastolic dysfunction, neutrophil-to-lymphocyte ratio, T-peak–to–T-end interval

Posted Date: June 24th, 2026

DOI: https://doi.org/10.21203/rs.3.rs-9788750/v1

License: This work is licensed under a Creative Commons Attribution 4.0 International License.
Read Full License

Additional Declarations: No competing interests reported.

Abstract

Background

Left ventricular diastolic dysfunction (LVDD) is echocardiographically defined, but its phenotype may reflect ambulatory hemodynamic stress, ventricular repolarization heterogeneity, and inflammation. We evaluated whether diastolic morning surge (DMS), T-peak–to–T-end (Tp-e) interval, and neutrophil-to-lymphocyte ratio (NLR) add discriminatory information for LVDD.

Methods

This cross-sectional study included adults evaluated between January 2025 and March 2026. Participants had complete 24-hour ambulatory blood pressure monitoring, 12-lead electrocardiography, differential blood count, and echocardiography. Exclusions included indeterminate diastolic function, LVEF < 50%, prior heart failure, moderate-to-severe valvular disease, persistent arrhythmia, CKD stage ≥ 3, or inflammatory/autoimmune disease. Definite LVDD was classified using the 2016 ASE/EACVI algorithm. Sequential logistic models were clinical, clinical plus ambulatory blood pressure, and final multidomain model incorporating DMS, Tp-e, and NLR.

Results

The cohort included 700 participants: 140 with definite LVDD and 560 with definite normal diastolic function. The LVDD group had more hypertension, diabetes mellitus, higher 24-hour systolic/diastolic pressures, attenuated nocturnal dipping, higher DBP load, greater DMS, longer Tp-e, and higher NLR. DMS (15.4 ± 6.5 vs. 9.5 ± 4.6 mmHg), Tp-e (92.5 ± 12.9 vs. 80.2 ± 9.5 ms), and NLR (2.69 ± 0.94 vs. 1.96 ± 0.71) were higher in LVDD (all $p < 0.001$). AUC improved from 0.72 to 0.77 and 0.87 (95% CI, 0.83–0.90) in the final model (ΔAUC + 0.10 vs. Model 2; $p < 0.001$), with Brier score 0.113 and calibration slope 1.00. Bootstrap validation yielded optimism-corrected AUC 0.86 and calibration slope 0.97.

Conclusions

DMS, Tp-e, and NLR provided incremental cross-sectional discriminatory information for echocardiographic LVDD, without replacing echocardiography.

INTRODUCTION

Circadian blood pressure dynamics expose the cardiovascular system to transient periods of increased hemodynamic load that are not fully captured by mean ambulatory blood pressure values. Diastolic morning surge (DMS) reflects the early-morning rise in diastolic pressure and may represent a repetitive diastolic hemodynamic stressor relevant to myocardial relaxation, ventricular loading conditions, and

remodeling along the heart failure with preserved ejection fraction (HFpEF) continuum. Left ventricular diastolic dysfunction (LVDD) is common in community-based populations and is considered an early structural and functional abnormality within the clinical pathway toward HFpEF (11). Structural remodeling, concentric geometry, and extracellular matrix expansion contribute to impaired myocardial relaxation and increased diastolic stiffness in HFpEF (12,32). Ambulatory blood pressure monitoring provides a more comprehensive assessment of dynamic hemodynamic burden than office blood pressure measurement alone (9), and circadian blood pressure variability, particularly exaggerated morning surge, has been associated with hypertension-mediated target-organ damage and adverse cardiovascular risk (10,18). Although systolic morning surge has been investigated more extensively, DMS may provide complementary information by capturing repetitive early-morning diastolic wall stress and peripheral vascular load.

Electrical and inflammatory pathways may further characterize the myocardial phenotype associated with LVDD. Ventricular repolarization heterogeneity, commonly assessed by prolongation of the T-peak–to–T-end (Tp-e) interval, has emerged as an electrocardiographic marker associated with adverse cardiovascular outcomes (26,28). Mechanical stress may also influence ventricular electrophysiology through mechano-electric coupling, providing a plausible link between dynamic hemodynamic load and repolarization abnormalities (27). In parallel, systemic inflammation contributes to myocardial stiffness, extracellular matrix remodeling, endothelial dysfunction, and microstructural alteration (29). The neutrophil-to-lymphocyte ratio (NLR), an accessible marker of systemic inflammatory activation, has been associated with hypertensive target-organ damage (16) and adverse outcomes in heart failure populations (17).

Taken together, these observations suggest that circadian diastolic hemodynamic stress, ventricular repolarization dispersion, and systemic inflammatory activation may represent complementary domains of myocardial vulnerability. However, it remains uncertain whether repolarization and inflammatory markers add discriminatory information beyond conventional clinical and ambulatory blood pressure variables for definite echocardiographic LVDD. Therefore, we constructed and internally validated a prespecified hierarchical model integrating clinical variables, ambulatory blood pressure parameters, DMS, Tp-e interval, and NLR. The aim of this study was to determine whether Tp-e interval and NLR, when added to ambulatory hemodynamic measures including DMS, improve cross-sectional discrimination of definite echocardiographic LVDD. Exploratory interaction analyses were also performed to assess whether the associations of electrical and inflammatory markers with LVDD differed according to the degree of circadian diastolic hemodynamic stress.

METHODS

Study Design and Population

This retrospective cross-sectional study was conducted using clinical data from consecutive adults evaluated between January 2025 and March 2026 at Ankara Bilkent City Hospital, a tertiary

cardiovascular center. The study protocol was approved by the Ethics Committee of Ankara Bilkent City Hospital (approval no. TABED 2-123-25), and the study was performed in accordance with the principles of the Declaration of Helsinki. Data were obtained through systematic review of electronic medical records.

Consecutive adults referred for 24-hour ambulatory blood pressure monitoring (ABPM) and transthoracic echocardiography during the study period were screened. Participants were eligible if they were aged ≥ 18 years and had complete 24-hour ABPM recordings with ≥ 70% valid measurements, standard 12-lead electrocardiography, laboratory data including differential blood counts, and guideline-directed echocardiographic assessment. All evaluations were performed within the same outpatient assessment period, and the interval between any two assessments did not exceed 7 days.

Exclusion criteria were incomplete or technically inadequate ABPM recordings, missing or inadequate echocardiographic assessment, unavailable or uninterpretable electrocardiographic data, missing laboratory data, left ventricular ejection fraction < 50%, prior diagnosis of heart failure, moderate-to-severe valvular heart disease, atrial fibrillation or other persistent arrhythmias, chronic kidney disease stage ≥ 3, and systemic inflammatory or autoimmune disease. Exclusion reasons were recorded hierarchically, and each participant was assigned to a single primary exclusion category to avoid double counting.

Of 5,145 screened individuals, 4,200 were excluded before eligibility confirmation or primary analysis because of incomplete ABPM recordings (n = 1,653), missing or inadequate echocardiography (n = 1,255), missing or uninterpretable electrocardiography (n = 821), missing laboratory data (n = 212), left ventricular ejection fraction < 50% (n = 31), prior heart failure (n = 22), moderate-to-severe valvular heart disease (n = 56), atrial fibrillation or other persistent arrhythmias (n = 51), chronic kidney disease stage ≥ 3 (n = 88), or systemic inflammatory or autoimmune disease (n = 11). Thus, 945 individuals fulfilled eligibility criteria and had complete datasets available for analysis (Fig. 1).

Footnote: A total of 5,145 consecutive adults were screened. Of these, 4,200 were excluded because of incomplete or technically inadequate ABPM recordings, missing or inadequate echocardiography, unavailable or uninterpretable ECG, missing laboratory data, LVEF < 50%, prior heart failure, moderate-to-severe valvular heart disease, persistent arrhythmia, chronic kidney disease stage ≥ 3, or systemic inflammatory/autoimmune disease. The remaining 945 participants had complete eligible datasets. Diastolic function was classified according to the 2016 ASE/EACVI algorithm. Among these, 245 participants were classified as having indeterminate diastolic function and were excluded from the primary analysis to preserve outcome specificity. The final primary analytic cohort included 700 participants: 560 with definite normal diastolic function and 140 with definite LVDD. ABPM, ambulatory blood pressure monitoring; ECG, electrocardiography; LVEF, left ventricular ejection fraction; LVDD, left ventricular diastolic dysfunction; ASE/EACVI, American Society of Echocardiography/European Association of Cardiovascular Imaging.

Diastolic function was classified according to the 2016 ASE/EACVI integrative algorithm. Among eligible participants, 245 individuals were classified as having indeterminate diastolic function and were excluded from the primary outcome model to preserve outcome specificity. The final primary analytic cohort consisted of 700 individuals, including 560 with definite normal diastolic function and 140 with definite LVDD.

Twenty-four-hour ABPM was performed using the HINGMED WBP-02A device. Standard 12-lead electrocardiograms were recorded using a Nihon Kohden system at a paper speed of 25 mm/s and a calibration of 10 mm/mV. Transthoracic echocardiography was performed using an Affiniti 50 system and interpreted by two cardiologists. Electrocardiographic repolarization indices, including Tp-e interval, QT interval, and QT dispersion, were measured offline by two cardiologists blinded to echocardiographic classification and clinical data.

Reproducibility of manual Tp-e measurements was assessed in a randomly selected subset of 50 ECGs. Manual electrocardiographic measurements showed high reproducibility, with an interobserver intraclass correlation coefficient of 0.88 and an intraobserver intraclass correlation coefficient of 0.89.

Ambulatory Blood Pressure Monitoring and Hemodynamic Variables

Twenty-four-hour ABPM was performed using a validated oscillometric device with measurements every 15 minutes during daytime (06:00–22:00) and every 30 minutes during nighttime (22:00–06:00). Recordings with ≥ 70% valid measurements were considered acceptable.

The following variables were derived:

- -Mean 24-hour systolic blood pressure (SBP)
- -Mean 24-hour diastolic blood pressure (DBP)
- -Daytime and nighttime SBP/DBP
- -Nocturnal systolic dipping (%) = [(daytime SBP − nighttime SBP) / daytime SBP] 100
- -24-hour DBP load (%)
- -24-hour average real variability (ARV) of DBP
- -Diastolic morning surge (DMS), defined as the difference between the mean DBP during the 2 hours after awakening and the lowest nighttime DBP
- -Systolic morning surge (SMS), defined analogously using SBP values

Awakening time was confirmed using patient diaries. In descriptive subgroup analyses, DMS ≥ 15 mmHg was considered elevated on the basis of prior observational studies evaluating diastolic morning surge. However, in all multivariable models, DMS was retained as a continuous variable to preserve statistical power and avoid information loss.

SBP dipping was calculated independently for each participant. In accordance with commonly used ABPM definitions, a dipping pattern was defined as a nocturnal reduction of ≥ 10% in systolic blood pressure, whereas a reduction of < 10% was classified as non-dipping.

Left Ventricular Diastolic Dysfunction Identification

Echocardiographic Assessment Framework

Left ventricular diastolic function was evaluated according to the 2016 joint recommendations of the American Society of Echocardiography and the European Association of Cardiovascular Imaging (ASE/EACVI) (1). All examinations were performed using standard parasternal and apical views with Doppler and tissue Doppler imaging obtained during quiet respiration.

The following parameters were assessed:

- -Mitral inflow early (E) and late (A) velocities
- -E/A ratio
- -Deceleration time
- -Septal and lateral early diastolic annular velocity (e')
- -Average E/e' ratio
- -Left atrial volume index (LAVI)
- -Tricuspid regurgitation (TR) peak velocity

All measurements were averaged over 3 cardiac cycles. Left ventricular ejection fraction was assessed by Simpson’s biplane method to confirm preserved systolic function.

Definition of Definite LVDD

Left ventricular diastolic function was assessed using the integrative algorithm recommended by the 2016 ASE/EACVI guidelines for patients with preserved ejection fraction. The 4 diagnostic variables evaluated were: (1) septal e' <7 cm/s or lateral e' <10 cm/s, (2) average E/e' ratio > 14, (3) LAVI > 34 mL/m², and (4) TR peak velocity > 2.8 m/s.

In accordance with guideline methodology, classification was based on a majority rule (> 50% of available parameters abnormal). When all 4 variables were measurable, LVDD was diagnosed if 3 or more criteria were abnormal, normal diastolic function was assigned if 3 or more were normal, and the presence of exactly 2 abnormal and 2 normal findings was classified as indeterminate diastolic function.

In cases in which only 3 parameters were available, such as non-measurable TR velocity, the same majority principle was applied: 2 or more abnormal findings were considered consistent with LVDD,

whereas 2 or more normal findings indicated normal diastolic function. No imputation of missing echocardiographic parameters was performed.

Handling of Indeterminate Diastolic Function

When exactly half of the available parameters met abnormal criteria, diastolic function was classified as indeterminate, consistent with guideline recommendations (1). This category reflects diagnostic uncertainty inherent to integrative echocardiographic algorithms and is common in epidemiologic cohorts. Participants classified as indeterminate were excluded from the primary modeling dataset and were evaluated separately in sensitivity analyses.

Electrocardiographic Analysis

Standard 12-lead electrocardiograms recorded at 25 mm/s and 10 mm/mV calibration were analyzed offline.

QT Interval and QT Dispersion

QT intervals were measured from the onset of the QRS complex to the end of the T wave, defined as the point at which the terminal limb of the T wave returned to the isoelectric baseline. QT intervals were measured in all 12 ECG leads, and QT dispersion was calculated as the difference between the maximum and minimum QT intervals across the 12-lead ECG. This approach was used to quantify spatial heterogeneity of ventricular repolarization.

T-peak–to–T-end (Tp-e) Interval

The Tp-e interval was measured manually on standard 12-lead electrocardiograms recorded at a paper speed of 25 mm/s and a calibration of 10 mm/mV. Measurements were obtained preferentially from lead V5; if V5 was not suitable because of low amplitude, indistinct morphology, or technical limitations, lead V4 or V6 was used. Tp-e was measured over 3 consecutive beats and the mean value was used for analysis. In the presence of a U wave, the end of the T wave was defined as the nadir between the T and U waves. ECGs with biphasic or poorly defined T waves in the candidate precordial leads were excluded from Tp-e measurement.

All Tp-e measurements were performed offline by 2 cardiologists blinded to echocardiographic findings and clinical data. Reproducibility was evaluated in a randomly selected subset of 50 ECGs, with repeat measurements performed 1 week apart. The measurement procedure showed high reproducibility, with an intraobserver intraclass correlation coefficient (ICC) of 0.89 (95% CI, 0.84–0.94) and an interobserver ICC of 0.88 (95% CI, 0.84–0.92). The Tp-e interval was analyzed as a marker of ventricular repolarization heterogeneity.

Laboratory Measurements

Peripheral venous blood samples were obtained after overnight fasting. Neutrophil and lymphocyte counts were measured using automated hematology analyzers. The neutrophil-to-lymphocyte ratio (NLR) was calculated as the absolute neutrophil count divided by the absolute lymphocyte count.

CRP was not entered into the primary hierarchical model to avoid post hoc marker substitution and to preserve the prespecified inflammatory component of the modeling framework.

Statistical Analysis

All statistical analyses were performed using IBM SPSS Statistics for Windows, version 25.0 (IBM Corp., Armonk, NY, USA), and R statistical software (R Foundation for Statistical Computing, Vienna, Austria). Data management, descriptive analyses, and baseline group comparisons were conducted in SPSS, whereas multivariable modeling, discrimination analysis, calibration assessment, and internal validation were performed in R.

Continuous variables were assessed for normality using the Shapiro–Wilk test together with visual inspection of histograms and Q–Q plots. Normally distributed variables are presented as mean ± standard deviation, whereas non-normally distributed variables are reported as median with interquartile range. Categorical variables are expressed as counts and percentages. Between-group comparisons were performed using the independent-samples Student's t test or Mann–Whitney U test, as appropriate. Categorical variables were compared using the chi-square test. Effect sizes were summarized using Cohen's d for normally distributed continuous variables, Cliff's δ for non-parametric comparisons, Cohen's h for pairwise comparisons of proportions, and Cramér's V for categorical associations where appropriate. All tests were two-sided, and a p value < 0.05 was considered statistically significant.

The primary objective of the statistical analysis was to evaluate whether ambulatory hemodynamic, electrocardiographic, and inflammatory markers provided complementary cross-sectional discriminatory information for definite echocardiographic left ventricular diastolic dysfunction. The primary outcome was definite LVDD, classified according to the 2016 ASE/EACVI diastolic function algorithm. Candidate predictors were selected a priori on the basis of biological plausibility, clinical relevance, and the prespecified multidomain structure of the study rather than data-driven variable selection. Continuous predictors were retained in their original measurement scales to preserve information and avoid arbitrary categorization.

A prespecified hierarchical logistic regression framework was used to evaluate incremental model performance across three sequential models.

Model 1 — Clinical model included age, sex, body mass index, diabetes mellitus, and current smoking status.

Model 2 — Clinical plus ABPM model included all variables in Model 1 plus 24-hour mean systolic blood pressure, 24-hour mean diastolic blood pressure, and nocturnal systolic dipping percentage.

Model 3 — Final multidomain model included all variables in Model 2 plus diastolic morning surge, T-peak–to–T-end interval, and neutrophil-to-lymphocyte ratio.

Smoking exposure was entered as current smoking status in the primary model to avoid collinearity and preserve model parsimony, whereas pack-years were reported descriptively. Hypertension history was not included in the primary multivariable model because the modeling framework prioritized contemporaneously measured ABPM-derived hemodynamic exposure over historical diagnostic labels. This approach was chosen to reduce conceptual overlap and to emphasize directly measured ambulatory blood pressure burden, circadian regulation, and morning surge dynamics.

The Tp-e interval was selected a priori as the primary electrocardiographic marker because it directly reflects ventricular repolarization heterogeneity as a standalone electrophysiological measure. Although Tp-e/QTc and related composite indices were evaluated descriptively, they were not incorporated into the main hierarchical model because QTc-based ratios may be influenced by heart rate-correction methods and denominator-related variability. The final model was therefore intentionally restricted to Tp-e as the primary electrical marker to preserve interpretability and model parsimony.

Model discrimination was quantified using the area under the receiver operating characteristic curve. Incremental changes in discrimination between sequential models were assessed using the DeLong test for correlated ROC curves. Classification performance was further summarized using sensitivity, specificity, positive predictive value, negative predictive value, positive likelihood ratio, and negative likelihood ratio at prespecified or data-derived operating thresholds, as appropriate.

Model calibration was assessed using the calibration intercept, calibration slope, and graphical calibration plots comparing predicted and observed probabilities across deciles of predicted probability. Overall model accuracy was evaluated using the Brier score. Internal validation was performed using bootstrap resampling with 1000 iterations to estimate optimism-corrected discrimination and calibration performance.

Model assumptions were examined before final interpretation. Linearity between continuous predictors and the log-odds of definite LVDD was assessed using fractional polynomial inspection and restricted cubic splines. When minor deviations from linearity were observed, linear terms were retained if there was no evidence of statistically significant nonlinearity and if model interpretability was improved. Multicollinearity was evaluated using variance inflation factors, with a variance inflation factor > 5 considered suggestive of problematic collinearity.

Two additional analyses were performed to examine the robustness and biological coherence of the primary findings. First, a sensitivity model additionally incorporating systolic morning surge was constructed to determine whether systolic circadian dynamics materially altered the associations or

discrimination of the final multidomain model. Second, exploratory interaction analyses were performed by adding multiplicative interaction terms for DMS × Tp-e and DMS × NLR to the final multidomain model. These interaction analyses were considered mechanistic extensions and were not part of the primary parsimonious model. Improvement in nested model fit after addition of interaction terms was assessed using the likelihood ratio test, and changes in discrimination were evaluated using ΔAUC with DeLong comparison.

The study was reported in accordance with the TRIPOD statement for transparent reporting of multivariable diagnostic and discrimination model research. Model coefficients, intercept values, full model specifications, and supplementary performance metrics are provided in the Supplementary Material to support transparency, reproducibility, and future external validation.

RESULTS

Baseline Clinical Characteristics

The study population consisted of 700 individuals, of whom 140 were classified as having definite LVDD. Demographic and clinical characteristics according to LVDD status are presented in Table 1. Individuals with LVDD had a higher prevalence of diabetes mellitus and a greater burden of hypertension history compared with those without LVDD. Age, sex distribution, body mass index, current smoking status, and pack-years were broadly comparable between groups; however, diabetes mellitus, and hypertension history were more frequent or higher in the LVDD group. Overall, clinical risk clustering was more prominent among participants with LVDD.

Ambulatory Hemodynamic Profile

Twenty-four–hour ABPM parameters are summarized in Table 2. Participants with LVDD exhibited consistently higher 24-hour systolic and diastolic pressures, as well as elevated daytime and nighttime values. Nocturnal dipping was attenuated, and diastolic blood pressure load and short-term variability (ARV) were significantly greater in the LVDD group. Importantly, diastolic morning surge (DMS) was substantially higher among individuals with LVDD. Although systolic morning surge (SMS) also differed between groups, its magnitude appeared less discriminative in hierarchical modeling. These findings suggest that dynamic diastolic load rather than mean systolic pressure alone characterizes the LVDD phenotype.

Echocardiographic Characteristics

Echocardiographic findings stratified by LVDD status are shown in Table 3. Consistent with the guideline-based definition of definite LVDD, the LVDD group demonstrated lower septal and lateral e' velocities, higher average E/e' ratio, and longer deceleration time, indicating impaired relaxation and higher filling pressures. Structural remodeling was also more prominent in this group, with higher left atrial volume index, greater relative wall thickness, and increased left ventricular mass index. Left ventricular ejection fraction was preserved in both groups.

Electrocardiographic Findings

Electrocardiographic parameters are detailed in Table 4. The Tp-e interval was significantly prolonged in individuals with LVDD, accompanied by higher Tp-e/QTc ratios and greater QT dispersion. QRS duration and conventional QTc showed only modest differences between groups. These results indicate greater ventricular repolarization heterogeneity in the LVDD phenotype.

Laboratory Parameters

Laboratory findings are summarized in Table 5. Neutrophil counts were higher in the LVDD group, while lymphocyte counts were comparable, resulting in significantly elevated NLR values. Inflammatory profile differences were consistent with a pro-inflammatory milieu in participants with diastolic dysfunction.

Hierarchical Multivariable Modeling

Hierarchical logistic regression results are presented in Table 6. The clinical model showed moderate discrimination for definite echocardiographic LVDD. Addition of ambulatory blood pressure parameters improved model performance, and the final multidomain model incorporating DMS, Tp-e interval, and NLR provided the strongest discrimination. Across the sequential modeling strategy, discrimination improved from an AUC of 0.72 in the clinical model to 0.87 in the final multidomain model after addition of DMS (Fig. 2), Tp-e interval, and NLR. The final model also showed good overall performance, with lower Brier score and calibration slopes close to unity. Bootstrap internal validation confirmed the stability of discrimination and calibration, with minimal evidence of overfitting.

Although later incremental gains were numerically smaller than the initial improvement achieved by adding ambulatory hemodynamic variables, they were directionally consistent and accompanied by preserved calibration and improved overall model accuracy.

Footnote (ROC Curve)

The receiver operating characteristic (ROC) curve illustrates the ability of the final cross-sectional discrimination model to distinguish participants with and without prevalent definite left ventricular diastolic dysfunction (LVDD). The area under the curve (AUC) summarizes overall discriminative performance across all possible classification thresholds. An AUC of 0.87 indicates good discrimination, whereas an AUC of 0.5 indicates chance-level performance and an AUC of 1.0 indicates perfect discrimination. The diagonal reference line represents the performance of a non-informative classifier.

Dominant Discriminatory Signals

Among the evaluated electrophysiological markers, indices reflecting ventricular repolarization dispersion showed the clearest separation between participants with and without LVDD. The Tp-e/QTc ratio showed the largest effect size among electrocardiographic parameters, followed by Tp-e interval and QT dispersion. Tp-e interval was longer in the LVDD group than in the normal diastolic function group

(92.5 ± 12.9 ms vs 80.2 ± 9.5 ms; d = 1.02; p < 0.001), and QT dispersion was also greater (40.9 ± 12.4 ms vs 32.3 ± 10.3 ms; d = 0.81; p < 0.001). In parallel, markers of diastolic hemodynamic burden demonstrated large between-group differences. DMS was substantially higher in the LVDD group (15.4 ± 6.5 mmHg vs 9.5 ± 4.6 mmHg; d = 1.07; p < 0.001), and diastolic blood pressure load showed strong separation between groups (35 ± 17% vs 20 ± 13%; d = 1.02; p < 0.001). These findings indicate that repolarization dispersion and diastolic hemodynamic load were the dominant signals differentiating the LVDD phenotype in this cohort.

Exploratory Interaction Analyses

Exploratory interaction analyses are summarized in Supplementary Table S6. DMS, Tp-e interval, and NLR were mean-centered before construction of interaction terms. In the centered interaction model, both cDMS × cTp-e and cDMS × cNLR were statistically significant, suggesting that the associations of repolarization heterogeneity and inflammatory activation with LVDD may vary according to the degree of diastolic morning hemodynamic stress. Addition of these interaction terms improved discrimination from 0.87 to 0.89 compared with the final multidomain model (ΔAUC = + 0.02; DeLong p = 0.04) and improved overall model fit on likelihood ratio testing (LR χ^2 = 6.2, df = 2, p = 0.041). These findings should be interpreted as exploratory and hypothesis-generating rather than as evidence of definitive biological interaction (Fig. 3).

Footnote

The calibration plot evaluates the agreement between model-fitted probabilities and observed proportions of definite LVDD. The 45° diagonal line represents perfect calibration, where model-fitted estimates correspond to observed event proportions. The apparent calibration curve reflects model performance in the derivation dataset, whereas the bootstrap-corrected curve accounts for potential optimism due to overfitting. Calibration was further summarized using the calibration slope and Brier score.

Sensitivity Analyses

Sensitivity analyses were conducted to evaluate the robustness of the primary modeling strategy with respect to the handling of indeterminate diastolic function and the inclusion of additional circadian hemodynamic parameters.

First, baseline characteristics of participants with indeterminate diastolic function were compared with both definite normal diastolic function and definite LVDD groups. Individuals with indeterminate diastolic function showed demographic characteristics, ambulatory blood pressure parameters, DMS values, and inflammatory indices that were largely closer to the definite normal group than to the definite LVDD group. In contrast, larger and more consistent differences were observed when the indeterminate group was compared with the definite LVDD group, particularly for diastolic load metrics, DMS, LAVI, tissue Doppler e' velocities, and repolarization markers.

Second, indeterminate cases were alternatively reclassified as normal diastolic function and as LVDD while preserving the same predictor structure. Model discrimination remained stable across these scenarios, with apparent AUC values of 0.87 in the primary analysis, 0.86 when indeterminate cases were classified as normal, and 0.85 when indeterminate cases were classified as LVDD. Optimism-corrected AUC values also remained stable at 0.86, 0.85, and 0.84, respectively. Calibration slopes remained close to unity, and calibration intercepts were near zero. Although the Brier score increased when indeterminate cases were classified as LVDD, overall model performance showed only modest variation. These findings indicate that exclusion of indeterminate cases did not materially inflate discrimination or compromise calibration.

Third, a sensitivity model incorporating systolic morning surge was evaluated. Although SMS showed a modest association with LVDD, its inclusion did not materially improve discrimination compared with the final multidomain model (ΔAUC + 0.01; p = 0.13), and calibration remained stable.

Taken together, these analyses indicate that the final multidomain discrimination model remained robust across alternative assumptions regarding indeterminate diastolic function and additional circadian hemodynamic parameters.

DISCUSSION

In this cross-sectional study integrating ambulatory hemodynamic indices, electrocardiographic repolarization markers, and inflammatory parameters, individuals with definite echocardiographic LVDD showed a distinct multimodal phenotype characterized by higher diastolic load, attenuated nocturnal systolic dipping, exaggerated diastolic morning surge, greater repolarization heterogeneity, and higher systemic inflammatory activity. Three main findings emerged. First, DMS provided discriminatory information beyond mean ambulatory blood pressure values and nocturnal dipping. Second, Tp-e interval and NLR remained associated with definite LVDD after multivariable adjustment and improved model discrimination. Third, exploratory interaction analyses suggested that the contribution of electrical and inflammatory markers may be more pronounced in the presence of greater diastolic morning surge, supporting a context-dependent myocardial vulnerability phenotype.

Diastolic Load and Circadian Hemodynamic Stress

Although systolic blood pressure has traditionally dominated cardiovascular risk assessment, sustained blood pressure load and impaired circadian regulation also have important pathophysiological consequences [9, 10, 18]. ABPM captures dynamic vascular stress more comprehensively than office blood pressure measurement alone [9, 18], and circadian blood pressure variability has been associated with hypertension-mediated target-organ damage [10, 18]. Morning blood pressure surge, particularly systolic surge, has been linked to stroke and vascular events [10, 24, 25]. However, DMS may provide complementary information by reflecting early-morning peripheral vascular load, diastolic wall stress, and repetitive increases in myocardial loading conditions [10, 19, 20].

Myocardial relaxation is sensitive to afterload, ventricular–arterial coupling, and diastolic wall stress [12, 13]. Repetitive early-morning diastolic surges may therefore contribute to higher filling pressures and concentric remodeling, both of which are central components of the HFpEF pathophysiological continuum [12, 13, 32]. In the present cohort, DMS improved discrimination beyond mean ambulatory pressures and nocturnal dipping, whereas SMS did not materially improve the final model. This suggests that circadian diastolic perturbation may capture a specific hemodynamic signal relevant to early abnormalities in myocardial relaxation.

Electrical Remodeling and Repolarization Dispersion

Ventricular repolarization heterogeneity, reflected by prolongation of the Tp-e interval, has been associated with structural heart disease, arrhythmic vulnerability, and adverse cardiovascular outcomes [15, 26, 28]. Myocardial fibrosis, altered electromechanical coupling, and microvascular dysfunction may contribute to abnormal repolarization indices [15, 27, 28], and these mechanisms also overlap with impaired relaxation, increased myocardial stiffness, and diastolic dysfunction [12, 13, 32].

In the final multidomain model, Tp-e interval remained associated with definite LVDD and contributed to improved discrimination. Mechanical stress may influence ventricular electrophysiology through mechano-electric coupling [27], providing a plausible explanation for the observed interaction between DMS and Tp-e. Because arrhythmic outcomes were not assessed, these findings should not be interpreted as evidence of arrhythmic risk prediction. Rather, they suggest that coexistence of exaggerated DMS and prolonged Tp-e may identify a phenotype characterized by both hemodynamic stress and electrical heterogeneity. This interpretation remains hypothesis-generating and requires confirmation in prospective rhythm-focused studies.

Inflammation and Diastolic Dysfunction

Chronic low-grade inflammation contributes to myocardial stiffness, extracellular matrix remodeling, endothelial dysfunction, and impaired diastolic reserve [29, 30, 32]. It may also promote microvascular rarefaction and altered myocardial energetics, both of which can contribute to elevated diastolic filling pressures [24, 32]. NLR is an accessible marker of systemic inflammatory activation and has been linked with hypertensive target-organ damage [16] and adverse outcomes in heart failure populations [17, 29].

In the present analysis, NLR provided additional discriminatory information beyond ambulatory hemodynamic and electrocardiographic variables. Although its incremental gain in AUC was modest, preserved calibration and reduction in Brier score suggest that inflammatory activation contributed reproducible information within the final multidomain framework. The exploratory interaction between DMS and NLR further supports the possibility that transient hemodynamic stress and inflammatory substrate may be interrelated in individuals with definite LVDD. Early-morning sympathetic activation, vascular reactivity, and adverse circadian hemodynamic responses may amplify myocardial stress in susceptible individuals [10, 19, 20, 25].

Cross-sectional Discrimination of Definite LVDD

Taken together, the findings support a layered pathophysiological framework consisting of a hemodynamic trigger, represented by DMS; an electrical substrate, reflected by repolarization dispersion; and an inflammatory milieu, reflected by NLR. Hierarchical modeling showed stepwise improvement in discrimination, while calibration remained stable after bootstrap correction [6]. Methodologically, modest incremental improvements may still be meaningful when accompanied by preserved calibration, improved overall accuracy, and biological coherence [2, 3, 6, 7].

The reclassification analyses involving indeterminate diastolic function produced only modest attenuation of discrimination without meaningful deterioration in calibration, supporting the stability of the model across alternative outcome definitions. Nevertheless, this study does not establish prognostic prediction for future HFpEF, atrial fibrillation, or arrhythmic events. Rather, it shows that integration of ABPM-derived circadian indices with electrocardiographic and inflammatory markers improves cross-sectional discrimination of prevalent definite echocardiographic LVDD within the derivation cohort. Clinical applicability requires prospective and external validation [24, 32].

The modeling strategy was intentionally designed to test whether electrical and inflammatory markers add information beyond ambulatory hemodynamic parameters, not to replace echocardiography or establish a clinical decision tool. Accordingly, the final model prioritized a parsimonious, biologically structured, and prespecified hierarchy. Twenty-four-hour SBP, 24-hour DBP, nocturnal systolic dipping, and DMS were selected as the core ambulatory hemodynamic variables because they represent overall pressure burden, circadian regulation, and early-morning diastolic stress. DBP load and DBP variability were not incorporated into the primary model because of conceptual and statistical overlap with 24-hour DBP and DMS. Similarly, although CRP differed descriptively between groups, NLR was retained as the prespecified inflammatory marker. Hypertension history was not included in the main model because contemporaneously measured ABPM-derived exposure was prioritized over historical diagnostic labeling.

The interaction findings should be interpreted as exploratory and supportive of contextual effect modification rather than proof of biological synergy. The stability of discrimination and calibration across alternative outcome-classification strategies argues against the primary findings being driven solely by the handling of indeterminate diastolic function.

Strengths and Methodological Considerations

This study has several methodological strengths. First, diastolic function was classified according to the 2016 ASE/EACVI integrative algorithm using a predefined majority-rule approach [1]. Indeterminate diastolic function was handled transparently through baseline comparisons and outcome-reclassification sensitivity analyses. Alternative outcome definitions resulted in only modest attenuation of discrimination and stable calibration, suggesting that model performance was not materially inflated by outcome selection.

Second, discrimination and calibration were internally validated using bootstrap correction, with preserved calibration slopes and limited optimism [2, 3, 6]. Third, incremental discrimination was evaluated using a prespecified hierarchical modeling strategy while preserving the same model structure across sensitivity analyses, reducing analytical flexibility and the risk of selective modeling [2, 3, 8].

LIMITATIONS

Several limitations should be acknowledged. First, this was a retrospective cross-sectional study conducted at a single tertiary cardiovascular center, which may limit generalizability. Although consecutive adults were screened and standardized measurement protocols were applied, residual selection bias cannot be excluded. Second, the cross-sectional design precludes causal inference; therefore, the associations between DMS, repolarization indices, inflammatory markers, and definite LVDD should not be interpreted as evidence of temporal sequence or mechanistic directionality.

Third, diastolic function classification relied on echocardiographic parameters obtained in routine clinical practice. Although guideline-based criteria were applied systematically, measurement variability and incomplete availability of some parameters, particularly TR velocity, may have introduced classification uncertainty. Fourth, external validation was not performed. Although bootstrap internal validation showed stable discrimination and calibration, independent validation in geographically and clinically distinct cohorts is required before transportability can be assumed [2, 3, 6, 7]. Fifth, inflammatory profiling was limited to routinely available laboratory indices; more specific biomarkers of myocardial fibrosis, extracellular matrix turnover, oxidative stress, or neurohormonal activation were not assessed.

Finally, the proposed framework should not be interpreted as a substitute for echocardiography or as a validated clinical decision tool. It represents a cross-sectional discrimination framework for prevalent definite echocardiographic LVDD within the derivation cohort. Despite these limitations, the consistency of findings across sensitivity analyses and the stability of discrimination and calibration metrics support the internal robustness of the reported associations.

CONCLUSIONS

In this ambulatory-based cohort, DMS, Tp-e interval, and NLR were associated with definite echocardiographic LVDD beyond conventional clinical variables and ambulatory blood pressure parameters. Their integration improved cross-sectional discrimination while preserving calibration across sensitivity analyses, including alternative outcome-classification strategies and bootstrap internal validation.

These findings support a multimodal framework in which prevalent definite LVDD is linked to the convergence of circadian diastolic hemodynamic stress, ventricular repolarization heterogeneity, and systemic inflammatory activation. Exaggerated DMS may act as a transient mechanical stressor that interacts with electrical and inflammatory substrates, potentially contributing to early myocardial remodeling along the HFpEF continuum [27, 32]. However, because the study was cross-sectional, the

model should be interpreted as a framework for discrimination of prevalent definite echocardiographic LVDD rather than as a prospective prediction tool. Longitudinal studies with external validation are needed to determine whether this integrated profile is associated with future clinical outcomes, including incident HFpEF or atrial fibrillation.

Abbreviations

ABPM, ambulatory blood pressure monitoring

AUC, area under the receiver operating characteristic curve

ARV, average real variability

ASE, American Society of Echocardiography

BMI, body mass index

CI, confidence interval

CRP, C-reactive protein

DBP, diastolic blood pressure

DMS, diastolic morning surge

E, early transmitral inflow velocity

e', early diastolic mitral annular velocity

E/A, ratio of early to late transmitral inflow velocities

EACVI, European Association of Cardiovascular Imaging

ECG, electrocardiography

HFpEF, heart failure with preserved ejection fraction

ICC, intraclass correlation coefficient

IQR, interquartile range

LAVI, left atrial volume index

LRT, likelihood ratio test

LVDD, left ventricular diastolic dysfunction

LVEF, left ventricular ejection fraction

LVMI, left ventricular mass index

NLR, neutrophil-to-lymphocyte ratio

OR, odds ratio

ROC, receiver operating characteristic

RWT, relative wall thickness

SBP, systolic blood pressure

SD, standard deviation

SMS, systolic morning surge

Tp-e, T-peak–to–T-end interval

TR, tricuspid regurgitation

TRIPOD, Transparent Reporting of a Multivariable Prediction Model for Individual Prognosis or Diagnosis

VIF, variance inflation factor

Declarations

Author Contributions

Conceptualization: A.C., H.O.

Methodology: A.C., H.O.

Data collection: A.C., H.O.

Formal analysis: A.C., H.O.

Writing – original draft: A.C., H.O.

Writing – review & editing: A.C.

Funding

This research received no external funding.

Conflicts of Interest

The authors declare no conflict of interest.

Ethics Approval

The study protocol was approved by the Ethics Committee of Ankara Bilkent City Hospital (Protocol No:TABED2-123-25; Date:1 DEC 2025) and conducted in accordance with the Declaration of Helsinki.

Data Availability Statement

The data that support the findings of this study are available from the corresponding author upon reasonable request.

References

1. Nagueh SF, Smiseth OA, Appleton CP, Byrd BF 3rd, Dokainish H, Edvardsen T, et al. Recommendations for the evaluation of left ventricular diastolic function by echocardiography. J Am Soc Echocardiogr. 2016;29(4):277–314. 10.1016/j.echo.2016.01.011.
2. Collins GS, Reitsma JB, Altman DG, Moons KGM. Transparent Reporting of a Multivariable Prediction Model for Individual Prognosis or Diagnosis (TRIPOD): the TRIPOD Statement. Ann Intern Med. 2015;162(1):55–63. 10.7326/M14-0697.
3. Moons KGM, Altman DG, Reitsma JB, Ioannidis JPA, Macaskill P, Steyerberg EW, et al. Transparent Reporting of a Multivariable Prediction Model for Individual Prognosis or Diagnosis (TRIPOD): Explanation and Elaboration. Ann Intern Med. 2015;162(1):W1–73. 10.7326/M14-0698.
4. Wolff RF, Moons KGM, Riley RD, Whiting PF, Westwood M, Collins GS, et al. PROBAST: a Tool to Assess the Risk of Bias and Applicability of Prediction Model Studies. Ann Intern Med. 2019;170(1):51–8. 10.7326/M18-1376.
5. Moons KGM, Wolff RF, Riley RD, Whiting PF, Westwood M, Collins GS, et al. PROBAST: a Tool to Assess Risk of Bias and Applicability of Prediction Model Studies: Explanation and Elaboration. Ann Intern Med. 2019;170(1):W1–33. 10.7326/M18-1377.
6. Van Calster B, McLernon DJ, van Smeden M, Wynants L, Steyerberg EW. Calibration: the Achilles heel of predictive analytics. BMC Med. 2019;17(1):230. 10.1186/s12916-019-1466-7.
7. Steyerberg EW, Vickers AJ, Cook NR, Gerds T, Gonen M, Obuchowski N, Pencina MJ, Kattan MW. Assessing the performance of prediction models: a framework for traditional and novel measures. *Epidemiology*. 2010;21(1):128–138. 10.1097/EDE.0b013e3181c30fb2. PMID: 20010215.
8. Riley RD, Ensor J, Snell KIE, Harrell FE Jr, Martin GP, Reitsma JB, et al. Calculating the sample size required for developing a clinical prediction model. BMJ. 2020;368:m441. 10.1136/bmj.m441.
9. Parati G, Stergiou GS, Dolan E, Bilo G. Blood pressure variability: clinical relevance and application. J Clin Hypertens (Greenwich). 2018;20(7):1133–7. 10.1111/jch.13304.
10. Bilo G, Grillo A, Guida V, Parati G. Morning blood pressure surge: pathophysiology, clinical relevance and therapeutic aspects. Integr Blood Press Control. 2018;11:47–56. 10.2147/IBPC.S130277.

11. Nayor M, Cooper LL, Enserro DM, Xanthakis V, Larson MG, Benjamin EJ, et al. Left ventricular diastolic dysfunction in the community: impact of diagnostic criteria on the burden, correlates, and prognosis. J Am Heart Assoc. 2018;7(11):e008291. 10.1161/JAHA.117.008291.
12. Kosmala W, Marwick TH. Asymptomatic left ventricular diastolic dysfunction: predicting progression to symptomatic heart failure. JACC Cardiovasc Imaging. 2020;13(1 Pt 2):215–27. 10.1016/j.jcmg.2018.10.039.
13. Wenzel JP, Bei der Kellen R, Magnussen C, Blankenberg S, Schrage B, Schnabel RB, et al. Diastolic dysfunction in individuals with and without heart failure with preserved ejection fraction. Clin Res Cardiol. 2022;111(4):416–27. 10.1007/s00392-021-01907-x.
14. Kim TH, Uhm JS, Joung B, Lee MH, Pak HN. Left ventricular diastolic dysfunction is associated with atrial remodeling and risk or presence of stroke in patients with paroxysmal atrial fibrillation. J Cardiol. 2016;68(2):104–9. 10.1016/j.jjcc.2015.10.008.
15. Li ZD, Bai XJ, Han LL, et al. Association between ventricular repolarization variables and cardiac diastolic function: a cross-sectional study of a healthy Chinese population. World J Clin Cases. 2019;7(8):940–50. 10.12998/wjcc.v7.i8.940.
16. Yu X, et al. NLR-A Simple Indicator of Inflammation for the Diagnosis of Left Ventricular Hypertrophy in Hypertension. Int Heart J. 2020. 10.1536/ihj.19-138.
17. Curran FM, Bhalraam U, Mohan M, Singh JS, Anker SD, Dickstein K, et al. Neutrophil-to-lymphocyte ratio and outcomes in patients with new-onset or worsening heart failure with reduced and preserved ejection fraction. ESC Heart Fail. 2021;8(4):3168–79. 10.1002/ehf2.13424.
18. Kario K. Perfect 24-h management of hypertension. J Hum Hypertens. 2017;31(4):231–43. 10.1038/jhh.2016.65.
19. Mokwatsi GG, Schutte AE, Mels CMC, Kruger R. Morning blood pressure surge in young black and white adults: the African-PREDICT study. J Hum Hypertens. 2019;33(1):22–33. 10.1038/s41371-018-0089-3.
20. Mokwatsi GG, Schutte AE, Mels CMC, Kruger R. Morning blood pressure surge relates to autonomic neural activity in young non-dipping adults: the African-PREDICT study. Heart Lung Circ. 2019;28(8):1197–205. 10.1016/j.hlc.2018.07.003.
21. Caf H, Dönmez Y, Çeliker Güler E, et al. Morning blood pressure surge is associated independently with orthostatic hypotension in hypertensive patients under treatment. Blood Press Monit. 2018;23(4):191–7. 10.1097/MBP.0000000000000326.
22. Koc AS, Gorgulu FF, Donmez Y, Icen YK. There is a significant relationship between morning blood pressure surge and increased abdominal aortic intima-media thickness in hypertensive patients. J Med Ultrason (2001). 2018;45(4):597–603. 10.1007/s10396-018-0877-y.
23. Mahfouz RA, Goda M, Galal I, Ghareb MS. Association of morning blood pressure surge with carotid intima-media thickness and cardiac dysfunction in patients with cardiac syndrome X. Blood Press. 2018;27(5):297–303. 10.1080/08037051.2018.1476056.

24. Xie JC, Lin YY, Liu XH, Zhao YC, Ma XY, Wang B, et al. Homocysteine is associated with exaggerated morning blood pressure surge in patients with acute ischemic stroke. J Stroke Cerebrovasc Dis. 2018;27(10):2650–6. 10.1016/j.jstrokecerebrovasdis.2018.05.032.
25. Di Gennaro F, D'Amato C, Morganti R, et al. Morning blood pressure surge is associated with autonomic neuropathy and peripheral vascular disease in patients with diabetes. J Hum Hypertens. 2020;34(7):495–504. 10.1038/s41371-019-0270-3.
26. Bombelli M, Maloberti A, Raina L, et al. Prognostic relevance of electrocardiographic Tpeak-Tend interval in the general and in the hypertensive population: data from the Pressioni Arteriose Monitorate E Loro Associazioni study. J Hypertens. 2016;34(9):1823–30. 10.1097/HJH.0000000000001005.
27. Saito Y, Yamada H, Kusunose K, et al. Noninvasive assessment of left-ventricular diastolic electromechanical coupling in hypertensive heart disease. J Echocardiogr. 2019;17(4):206–12. 10.1007/s12574-019-00421-4.
28. Tse G, Gong M, Wong WT, et al. The Tpeak-Tend interval as an electrocardiographic risk marker of arrhythmic and mortality outcomes: a systematic review and meta-analysis. Heart Rhythm. 2017;14(8):1131–7. 10.1016/j.hrthm.2017.05.031.
29. Boralkar KA, Kobayashi Y, Amsallem M, et al. Value of neutrophil to lymphocyte ratio and its trajectory in patients hospitalized with acute heart failure and preserved ejection fraction. Am J Cardiol. 2020;125(2):229–35. 10.1016/j.amjcard.2019.10.020.
30. Hou M, Cao L, Ding Y, Chen Y, Wang B, Shen J, et al. Neutrophil to lymphocyte ratio is increased and associated with left ventricular diastolic function in newly diagnosed essential hypertension children. Front Pediatr. 2021;9:576005. 10.3389/fped.2021.576005.
31. Zhang H, Zhang Y, Li X, Bi Y, Wang X, Li J. Neutrophil-to-lymphocyte ratio is associated with left ventricular diastolic dysfunction in patients with overt hyperthyroidism. Front Endocrinol (Lausanne). 2022;13:906947. 10.3389/fendo.2022.906947.
32. Paulus WJ, Tschöpe C. A novel paradigm for heart failure with preserved ejection fraction: comorbidities drive myocardial dysfunction and remodeling through coronary microvascular endothelial inflammation. J Am Coll Cardiol. 2013;62(4):263–71. 10.1016/j.jacc.2013.02.092.

Tables

Table 1. Baseline Demographics and Clinical Characteristics According to LVDD Status

Variable	LVDD (−) (n=560)	LVDD (+) (n=140)	Test Statistic	p value	Effect Size
Age, years	43.2 ± 4.1	43.9 ± 4.3	t=-1.88	0.060	d=0.17
Male sex, n (%)	363 (64.8%)	95 (67.8%)	χ^2=0.42	0.52	V=0.025
BMI, kg/m²	25.4 ± 3.9	25.7 ± 4.1	t=−0.79	0.43	d=0.07
Hypertension history, n(%)	159 (28.4%)	72 (51.4%)	χ^2=31.2	<0.001	V=0.21
Diabetes mellitus, n(%)	55 (9.8%)	29 (20.7%)	χ^2=12.6	<0.001	V=0.13
Current smoking (n%)	234 (41.8%)	61 (43.6%)	χ^2=0.16	0.69	V=0.015
Pack-years	27.9 ± 3.7	28.2 ± 4.0	t=−0.85	0.39	d=0.08

Abbreviations:

LVDD, left ventricular diastolic dysfunction; BMI, body mass index.

Footnote:

Continuous variables are presented as mean ± standard deviation (SD) and were compared using the independent samples t-test. Categorical variables are presented as number (percentage) and were compared using the chi-square (χ^2) test. Effect size for continuous variables is expressed as Cohen's d, and for categorical variables as Cramér's V. A two-sided p value <0.05 was considered statistically significant.

Table 2. Ambulatory blood pressure monitoring parameters according to LVDD status

Parameter	LVDD (−)	LVDD (+)	Test	p	Effect Size
24h SBP	121.6 ± 9.5	128.9 ± 10.1	t=−8.44	<0.001	d=0.75
24h DBP	75.9 ± 6.3	79.8 ± 6.9	t=−6.81	<0.001	d=0.61
Daytime SBP	127.9 ± 10.2	133.7 ± 11.6	t=−6.27	<0.001	d=0.58
Daytime DBP	79.3 ± 7.1	84.2 ± 7.8	t=−7.33	<0.001	d=0.71
Nighttime SBP	111.4 ± 8.7	115.9 ± 9.4	t=−5.68	<0.001	d=0.52
Nighttime DBP	65.5 ± 5.4	71.2 ± 6.6	t=−10.3	<0.001	d=0.91
Nocturnal systolic dipping, %	12.4 ± 5.2	9.1 ± 5.0	t=6.73	<0.001	d=0.65
DBP load	20 ± 13	35 ± 17	t=−10.79	<0.001	d=1.02
DBP ARV	7.2 ± 1.8	8.7 ± 2.3	t=−8.18	<0.001	d=0.71
DMS (DBP)	9.5 ± 4.6	15.4 ± 6.5	t=−11.6	<0.001	d=1.07
SMS (SBP)	17.2 ± 7.3	24.6 ± 9.0	t=−9.64	<0.001	d=0.85

Abbreviations:

ABPM, ambulatory blood pressure monitoring; SBP, systolic blood pressure; DBP, diastolic blood pressure; ARV, average real variability; DMS, diastolic morning surge; SMS, systolic morning surge; LVDD, left ventricular diastolic dysfunction.

Footnote:

Values are presented as mean ± standard deviation (SD). Group comparisons were performed using the independent samples t-test. Effect size for continuous variables is expressed as Cohen’s d. A two-sided p value <0.05 was considered statistically significant. Nocturnal dipping represents the percentage decline in nighttime blood pressure relative to daytime values. DMS and SMS were calculated as the difference between the mean blood pressure during the first two hours after awakening and the lowest nighttime blood pressure.

Table 3. Echocardiographic parameters according to LVDD status

Parameter	LVDD (−)	LVDD (+)	Test	p	Effect Size
E velocity	75.8 ± 12.9	70.4 ± 14.6	t=3.96	<0.001	d=0.39
A velocity	61.1 ± 12.1	73.8 ± 15.4	t=−10.4	<0.001	d=0.93
E/A ratio	1.27 ± 0.33	0.97 ± 0.27	t=11.7	<0.001	d=1.00
Deceleration time	184 ± 35	215 ± 43	t=−9.0	<0.001	d=0.82
e’ septal	8.6 ± 1.5	6.8 ± 1.3	t=13.4	<0.001	d=1.24
e’ lateral	11.3 ± 2.0	8.9 ± 1.8	t=14.7	<0.001	d=1.34
Average E/e’	8.5 ± 2.1	11.1 ± 2.3	t=12.6	<0.001	d=1.20
TR velocity	2.26 ± 0.23	2.65 ± 0.27	t=14.0	<0.001	d=1.43
LAVI	25.1 ± 5.5	33.9 ± 7.1	t=13.7	<0.001	d=1.25
IVS thickness	9.2 ± 1.0	10.4 ± 1.1	t=−11.4	<0.001	d=1.17
PW thickness	9.0 ± 1.0	10.2 ± 1.1	t=−11.2	<0.001	d=1.14
Relative wall thickness	0.37 ± 0.04	0.41 ± 0.06	t=−8.41	<0.001	d=0.76
LVMI	85.4 ± 15.3	93.7 ± 17.2	t=−6.2	<0.001	d=0.55
LVEF	62.2 ± 4.6	61.3 ± 5.0	t=1.97	0.049	d=0.19

Abbreviations: E, early diastolic transmitral flow velocity; A, late diastolic transmitral flow velocity; E/A, ratio of early to late transmitral flow velocities; e', early diastolic mitral annular velocity; E/e', ratio of transmitral E velocity to mitral annular e' velocity; TR, tricuspid regurgitation; LAVI, left atrial volume index; IVS, interventricular septum; PW, posterior wall; RWT, relative wall thickness; LVMI, left ventricular mass index; LVEF, left ventricular ejection fraction; LVDD, left ventricular diastolic dysfunction.

Footnote: Values are presented as mean ± standard deviation (SD). Comparisons between groups were performed using the independent samples t-test. Effect size for continuous variables is expressed as Cohen’s d. LAVI and LVMI were indexed to body surface area. A two-sided p value <0.05 was considered statistically significant.

Table 4. Electrocardiographic parameters according to LVDD status

Parameter	LVDD (−)	LVDD (+)	Test	p	Effect Size
Heart rate	71.6 ± 8.1	74.6 ± 8.4	t=−3.72	<0.001	d=0.36
QRS duration	88.3 ± 9.2	90.1 ± 9.5	t=−2.02	0.043	d=0.19
QT (raw)	385 ± 23	391 ± 24	t=−2.95	0.003	d=0.26
QTc	409 ± 17	416 ± 20	t=−3.85	<0.001	d=0.37
Tp-e	80.2 ± 9.5	92.5 ± 12.9	t=−11.4	<0.001	d=1.02
Tp-e/QTc	0.191 ± 0.020	0.224 ± 0.027	t=−12.8	<0.001	d=1.21
QT dispersion	32.3 ± 10.3	40.9 ± 12.4	t=−8.9	<0.001	d=0.81

Abbreviations:

ECG, electrocardiography; QT, QT interval; QTc, heart rate–corrected QT interval; Tp-e, T-peak to T-end interval; Tp-e/QTc, ratio of T-peak to T-end interval to corrected QT interval; LVDD, left ventricular diastolic dysfunction.

Footnote:

Values are presented as mean ± standard deviation (SD). Group comparisons were performed using the independent samples t-test. Effect size for continuous variables is expressed as Cohen's d. QTc was calculated using Bazett's correction formula. QT dispersion was defined as the difference between the maximum and minimum QT intervals across the 12-lead ECG. A two-sided p value <0.05 was considered statistically significant.

Tablo 5. Laboratory Parameters

Parameter	LVDD (−)	LVDD (+)	Test	p	Effect Size
Neutrophils	4.0 ± 1.1	4.9 ± 1.3	t=−8.4	<0.001	d=0.79
Lymphocytes	2.0 ± 0.6	2.0 ± 0.5	t=0.18	0.85	d=0.02
NLR	1.96 ± 0.71	2.69 ± 0.94	t=−10.2	<0.001	d=0.89
CRP	2.5 (1.1-4.9)	3.4 (2.5-9.1)	Mann–Whitney U	<0.001	Cliff's δ=0.44
Creatinine	0.91 ± 0.13	0.94 ± 0.14	t=−2.51	0.012	d=0.22
Fasting glucose	96 ± 13	101 ± 16	t=−4.1	<0.001	d=0.33
HbA1c	5.5 ± 0.5	5.8 ± 0.6	t=−5.1	<0.001	d=0.49

Abbreviations:

NLR, neutrophil-to-lymphocyte ratio; CRP, C-reactive protein; HbA1c, glycated hemoglobin; LVDD, left ventricular diastolic dysfunction.

Footnote:

Values are presented as mean ± standard deviation (SD) for normally distributed variables and as median (interquartile range, IQR) for non-normally distributed variables. Group comparisons for continuous variables were performed using the independent samples t-test. CRP levels were compared using the Mann–Whitney U test due to non-normal distribution. Effect size for parametric comparisons is expressed as Cohen's d, and for non-parametric comparisons as Cliff's δ. A two-sided p value <0.05 was considered statistically significant.

Table 6. Sequential model performance for cross-sectional discrimination of definite LVDD

Model	Variables included	AUC (95% CI)	ΔAUC vs previous model	DeLong p value	Apparent Brier score	Apparent calibration slope
Model 1 — Clinical model	Age, sex, BMI, diabetes mellitus, current smoking	0.72 (0.67–0.77)	—	—	0.152	0.97
Model 2 — Clinical + ABPM model	Model 1 + 24-h SBP, 24-h DBP, nocturnal systolic dipping	0.77 (0.72–0.82)	+0.05	0.004	0.139	0.95
Model 3 — Final multidomain model	Model 2 + DMS, Tp-e interval, NLR	0.87 (0.83–0.90)	+0.10	**<0.001**	0.113	1.00

Bootstrap internal validation of the final multidomain model

Model	Optimism-corrected AUC	Corrected calibration slope
Final multidomain model	0.86	0.97

Abbreviations:

ABPM, ambulatory blood pressure monitoring; AUC, area under the receiver operating characteristic curve; BMI, body mass index; DBP, diastolic blood pressure; DMS, diastolic morning surge; LVDD, left ventricular diastolic dysfunction; NLR, neutrophil-to-lymphocyte ratio; SBP, systolic blood pressure; Tp-e, T-peak–to–T-end interval.

Footnote:

Sequential multivariable logistic regression models were constructed to evaluate the incremental cross-sectional discriminatory contribution of ambulatory hemodynamic, electrocardiographic, and inflammatory markers for definite LVDD. Model 1 included clinical covariates. Model 2 additionally incorporated ABPM-derived hemodynamic variables. Model 3 represented the final multidomain model and added DMS, Tp-e interval, and NLR. Discrimination was quantified using AUC. Incremental differences in AUC were compared using the DeLong test for correlated ROC curves. Overall model accuracy was assessed using the Brier score, and calibration was summarized using the calibration slope. Internal validation of the final multidomain model was performed using bootstrap resampling with 1000 iterations. Full regression coefficients and intercept values for the final model are provided in Supplementary Table S1.

Figures

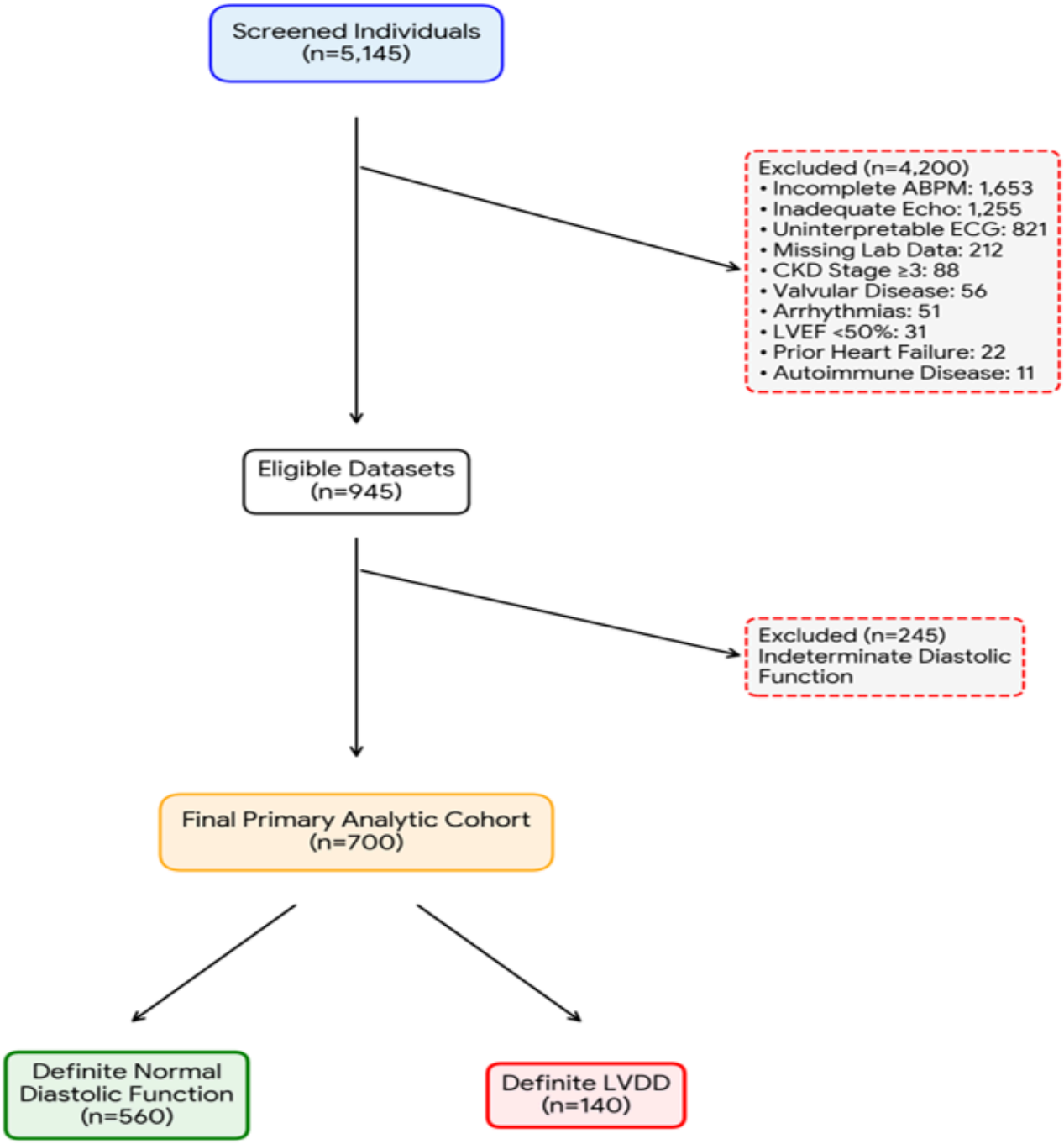


Figure 1

Study flow chart of patient selection and diastolic function classification.

Footnote:A total of 5,145 consecutive adults were screened. Of these, 4,200 were excluded because of incomplete or technically inadequate ABPM recordings, missing or inadequate echocardiography, unavailable or uninterpretable ECG, missing laboratory data, LVEF <50%, prior heart failure, moderate-to-severe valvular heart disease, persistent arrhythmia, chronic kidney disease stage ≥3, or systemic inflammatory/autoimmune disease. The remaining 945 participants had complete eligible datasets. Diastolic function was classified according to the 2016 ASE/EACVI algorithm. Among these, 245

participants were classified as having indeterminate diastolic function and were excluded from the primary analysis to preserve outcome specificity. The final primary analytic cohort included 700 participants: 560 with definite normal diastolic function and 140 with definite LVDD. ABPM, ambulatory blood pressure monitoring; ECG, electrocardiography; LVEF, left ventricular ejection fraction; LVDD, left ventricular diastolic dysfunction; ASE/EACVI, American Society of Echocardiography/European Association of Cardiovascular Imaging.

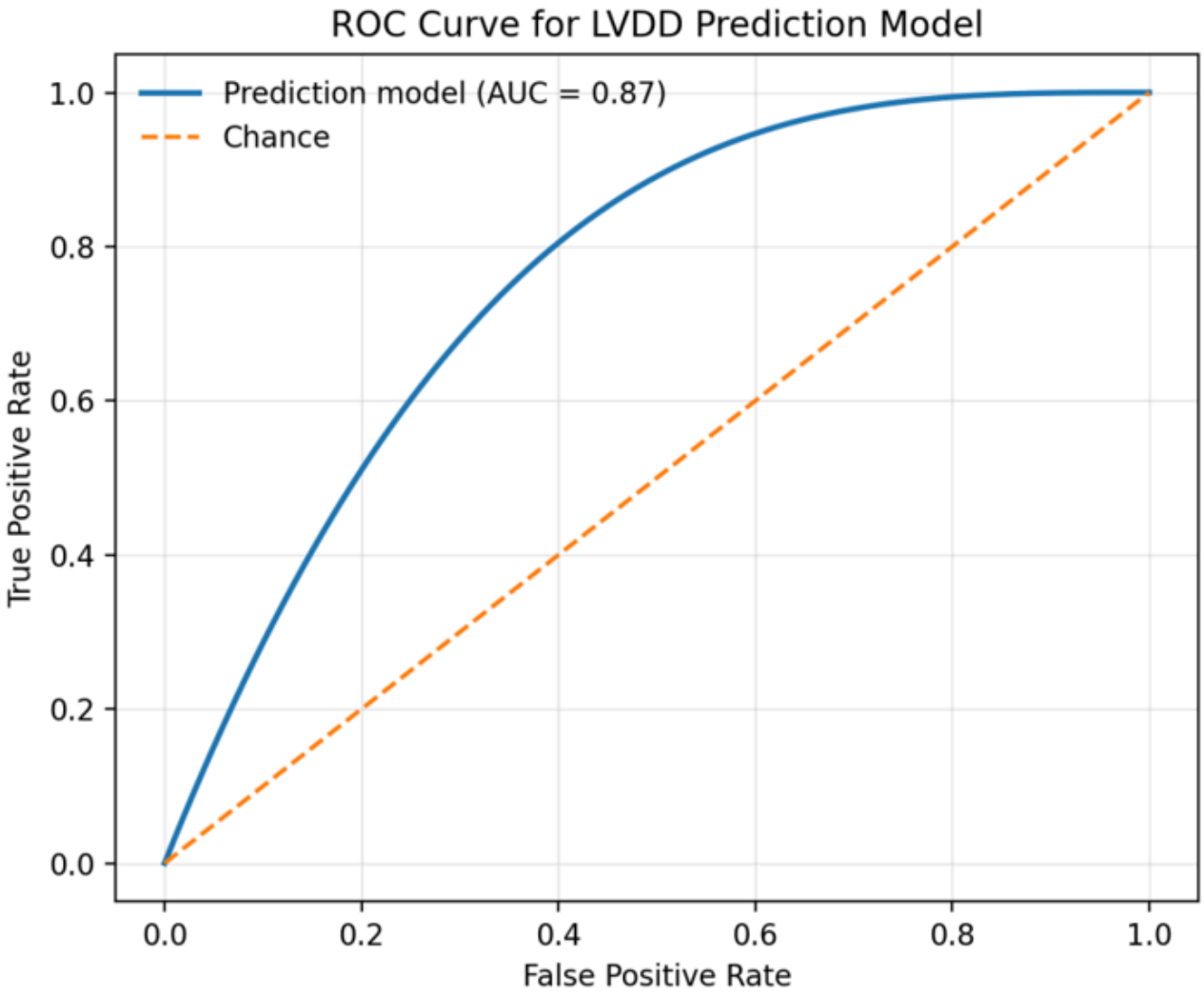


Figure 2

Receiver operating characteristic (ROC) curve of the final cross-sectional discrimination model for definite left ventricular diastolic dysfunction (LVDD).

Footnote (ROC Curve): The receiver operating characteristic (ROC) curve illustrates the ability of the final cross-sectional discrimination model to distinguish participants with and without prevalent definite left ventricular diastolic dysfunction (LVDD). The area under the curve (AUC) summarizes overall discriminative performance across all possible classification thresholds. An AUC of 0.87 indicates good discrimination, whereas an AUC of 0.5 indicates chance-level performance and an AUC of 1.0 indicates

perfect discrimination. The diagonal reference line represents the performance of a non-informative classifier.

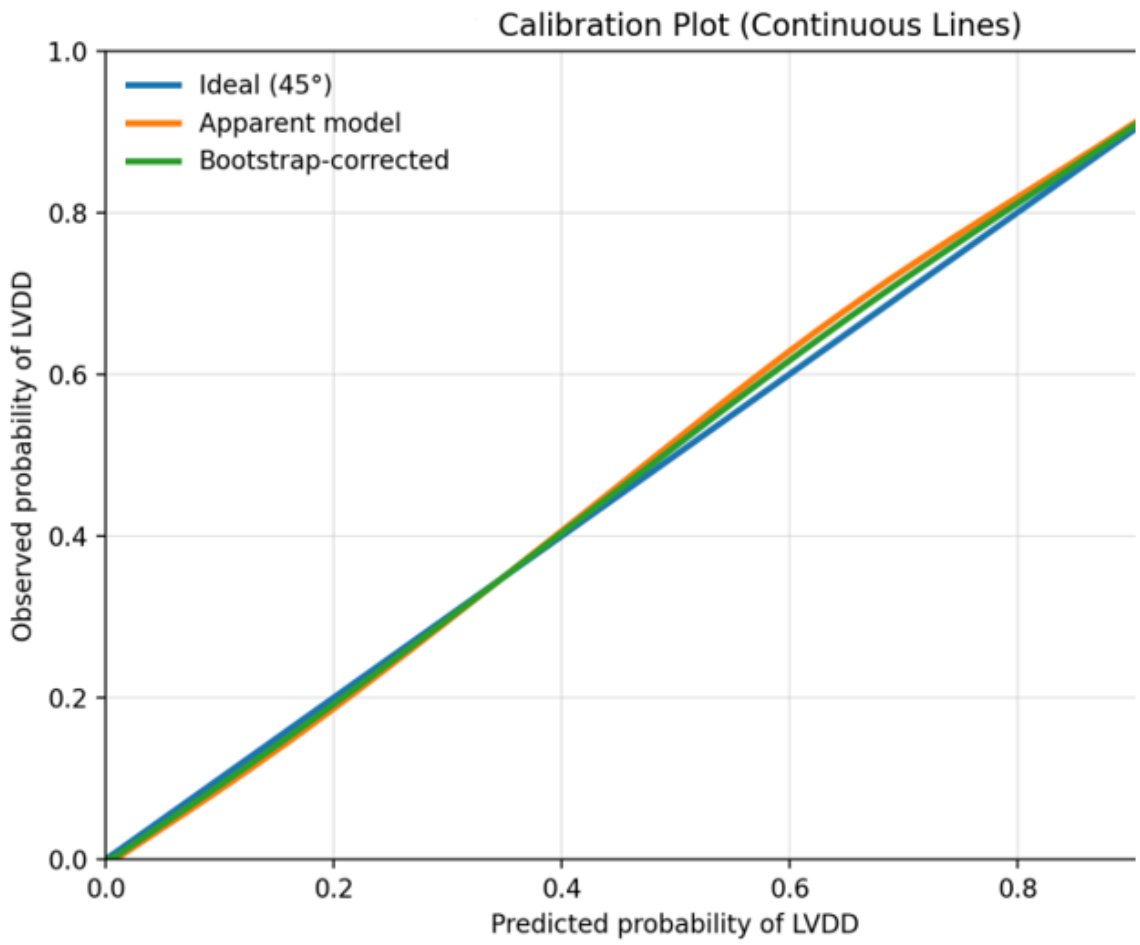


Figure 3

Calibration plot for the final model discriminating definite left ventricular diastolic dysfunction (LVDD).

Footnote: The calibration plot evaluates the agreement between model-fitted probabilities and observed proportions of definite LVDD. The 45° diagonal line represents perfect calibration, where model-fitted estimates correspond to observed event proportions. The apparent calibration curve reflects model performance in the derivation dataset, whereas the bootstrap-corrected curve accounts for potential optimism due to overfitting. Calibration was further summarized using the calibration slope and Brier score.

Supplementary Files

This is a list of supplementary files associated with this preprint. Click to download.

- SUPPLEMENTARYMATERIALDMSSONBMC.docx